AIP Journal of Applied Physics

Dark defects in InGaAsP/InP double heterostructure lasers under accelerated aging

M. Fukuda, K. Wakita, and G. Iwane

Citation: Journal of Applied Physics **54**, 1246 (1983); doi: 10.1063/1.332186
View online: http://dx.doi.org/10.1063/1.332186
View Table of Contents: http://scitation.aip.org/content/aip/journal/jap/54/3?ver=pdfcov
Published by the AIP Publishing

Dark defects in InGaAsP/InP double heterostructure lasers under accelerated aging

M. Fukuda, K. Wakita, and G. Iwane
Musashino Electrical Communication Laboratory, Nippon Telegraph and Telephone Public Corporation, Musashino-shi, Tokyo 180, Japan

(Received 29 September 1982; accepted for publication 3 November 1982)

Degradation modes due to dark defects under accelerated aging for InGaAsP/InP double heterostructure lasers are investigated by monitoring pulse threshold current, leak current, absorption coefficient, gain factor, and electroluminescence topograph. Most of the dark defects are dark spot defects (DSD's) and there are only few ⟨100⟩ dark line defects. At the initial stage of the degradation, these dark defects scarcely absorb the emitted light, and the reduction of gain factor causes the increase of pulse threshold current. After this stage, dark defects begin to act as absorber of the emitted light. The generation time of such DSD's strongly depends on the injected current density but only weakly on the junction temperature in the range of 25 ° to 250 °C. The activation energies for the generation time of the first dark spot defect and the growing speed of ⟨100⟩ dark line defects are estimated to be 0.16 and 0.2 eV, respectively.

PACS numbers: 42.55.Px, 85.30.De

I. INTRODUCTION

InGaAsP/InP double heterostructure (DH) lasers are important as optical sources for optical fiber communication. High reliability is required in order to use them as optical sources for long-haul and undersea optical fiber transmission systems. Recently, observation of dark spot defects (DSD's), ⟨110⟩ dark line defects (DLD's), and dark region have been reported for InGaAsP/InP DH lasers and light emitting diodes (LED's).[1–6] Degradation modes related to dark defects, however, have not been made clear.

The authors previously reported that rapid degradation and self-sustained pulsation, both of which were associated with DSD's or ⟨100⟩ DLD's, occurred under accelerated aging in InGaAsP/InP DH lasers.[3,7] A Ga- and As-rich region and sometimes dislocation loops with platelike precipitates were observed at the DSD's by electron probe microanalyzer and transmission electron microscope in the InGaAsP/InP DH lasers aged for a few hundred hours under high acceleration.[8,9] Moreover, the origins of these DSD's were shown to be in the vicinity of the active layer.[3,8]

The present work reports on the influence of dark defects on lasing characteristics and the dependence of DSD's generation time and the growing speed of ⟨100⟩ DLD's on injection current and junction temperature for InGaAsP/InP DH lasers. The degree of degradation was investigated through the change in pulse threshold current, current-voltage characteristics, absorption coefficient, gain factor, as well as an electroluminescence (EL) topograph of the active region. As a result, it is found that the appearance of dark defects in lasers causes the increase of pulse threshold current and recombination ($2kT$ component) leak current under forward bias, but the dark defects hardly act as absorber of emitted light at the initial stage of degradation. The dependence of dark defects generation time and their growing speed on operating conditions are discussed. The generation time of DSD's is found to be strongly dependent on the current density. The activation energies of DSD generation time and the growing speed of ⟨100⟩ DLD are estimated to be 0.16 and 0.2 eV, respectively.

II. EXPERIMENTAL PROCEDURES

InGaAsP/InP DH lasers used were conventional Zn-diffused planar stripe lasers with lasing wavelengths at 1.29 and 1.55 μm. The samples were taken from three wafers for lasers lasing at 1.29 μm and from two wafers for lasers lasing at 1.55 μm. Wafers were composed of four epilayers: an n-type cladding layer (Ge-doped for lasers lasing at 1.29 μm and Sn-doped for ones lasing at 1.55 μm, 4–5 μm thick), an active layer ($\sim$0.2 μm thick), a p-type cladding layer (Cd-doped for ones lasing at 1.29 μm and Zn-doped for ones lasing at 1.55 μm, $\sim$1.5 μm thick), and an n-type InGaAsP contact layer (Ge-doped for ones lasing at 1.29 μm and, Sn-doped for ones lasing at 1.55 μm, $\sim$0.7 μm thick.)[10] They were sequentially grown by liquid phase epitaxy on an (001) InP substrate. Active layers were undoped InGaAsP and cavity lengths were 200 μm with planar stripe width of 5–25 μm. The etch pit density of the InP substrate was about 4×10^4 cm^{-2}. The p- and n-side electrode were Au/Zn and Au/Ge/Ni, respectively. Initial pulse threshold currents were between 90 and 300 mA. In order to observe the EL topograph of the active region through the InP substrate, a part of the n-side electrode for each sample was removed along the stripe.[11] These samples were mounted p-side down on diamond heat sinks with Au-Sn solder, or were clamped to gold-plated copper heat sinks with phospher bronze springs without solder. All samples were preselected to be free of DSD's or DLD's by EL observation. The aging was carried out at forward current densities of 5, 10, and 15 kA/cm^2 with junction temperatures of about 30, 130, and 250 °C. For clamped samples, the junction temperatures were estimated from the differences of EL spectra peaks under pulse and cw operation, and the temperatures for mounted samples were estimated from thermal resistances and ambient temperature. Pulse threshold current and current-voltage

 0021-8979/83/031246-05$02.40

characteristics were monitored at 25 °C by interrupting the aging. At the same time, the absorption coefficient and gain factor were determined by measuring the threshold current density as a function of cavity loss.[12] The cavity loss of samples was changed by immersing the samples in methyl alcohol, benzene, and methylene iodide at 25 °C.

III. AGING CHARACTERISTICS

Relative pulse threshold currents, $I_{th}(t)/I_{th}(0)$, as a function of aging time t is shown in Fig. 1. As DSD's and ⟨100⟩ DLD's grew and their numbers increased in the EL topograph, pulse threshold current increased. However, the numbers of DSD and ⟨100⟩ DLD saturated after some aging, and the pulse threshold currents also had a tendency to saturate. For example, under injected current density of 10 kA/cm^2 and junction temperature of 250 °C, the numbers of DSD's and ⟨100⟩ DLD's saturated within about 50 h and those numbers never increased in the succeeding aging over 300 h. On the other hand, there were some samples in which no DSD's or DLD's are observed and their pulse threshold currents hardly changed even after 3000-h aging. Only samples having the origins of dark defects seem to degrade during aging. In other words, the origins of the dark defects are not created during aging within our experimental range.

IV. DEGRADATION MODE

It was reported that dark defects act as an absorber of emitted light in AlGaAs/GaAs DH lasers through the analyses using the absorption coefficient and the gain factor.[13,14] By using the same techniques, the degradation mode due to dark defects was experimentally investigated in InGaAsP/InP DH lasers. The absorption coefficient α, gain factor β, and threshold current density J_{th} are related to each other as follows:

$$\beta\cdot(J_{th}/d)^n = \alpha + (1/L)\ln(1/R), \tag{1}$$

where L and R are cavity length and reflectivity of mirror facet, respectively, and d is the thickness of an active layer. Thus, values α and β can be determined experimentally from the change of J_{th} as a function of the facet reflectivity.[12] The changes of absorption coefficient and gain factor versus the increase of pulse threshold current due to DSD's and DLD's, normalized by their initial values, are shown in Fig. 2. The values of n obtained from the experiments by a curve fitting were about 1. This value of n was nearly constant during degradation in all samples. The initial values of α were between 20 and 40 cm^{-1}.

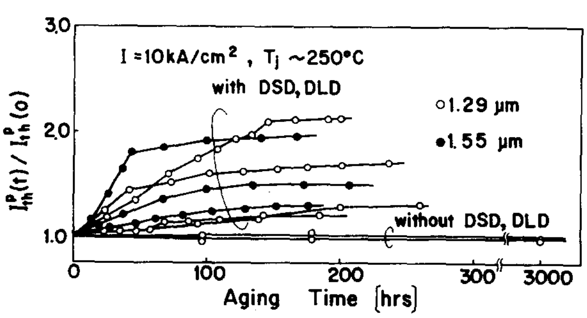

FIG. 1. Change in pulse threshold current, normalized by their initial value, as a function of aging time.

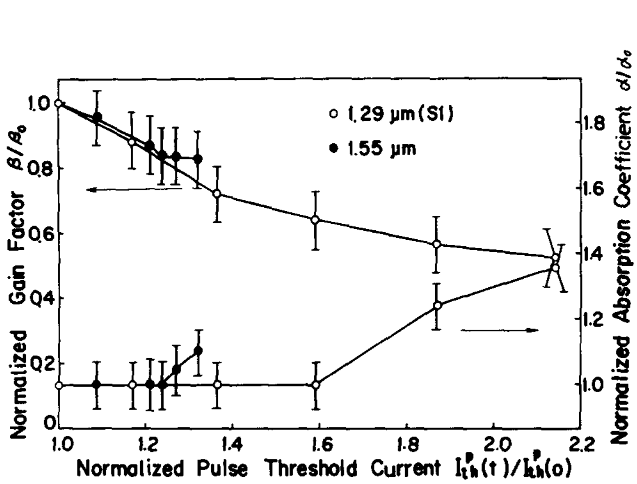

FIG. 2. Typical change in absorption coefficient and gain factor as a function of pulse threshold current. Driving current and junction temperature are 10 kA/cm^2 and 250 °C, respectively.

At the initial stage of degradation, the absorption coefficient α scarcely changes, whereas the gain factor β gradually decreases. This indicates that dark defects scarcely act as an absorber of emitted light in the initial stage. The number of dark defects saturates in this stage. After some degradation, the absorption coefficient begins to increase. As the absorption coefficient increased, self-sustained pulsations were observed in a few samples lasing at 1.29 μm.[7]

At the initial stage of the degradation, leak current increases under forward bias. The increment of pulse thresh-

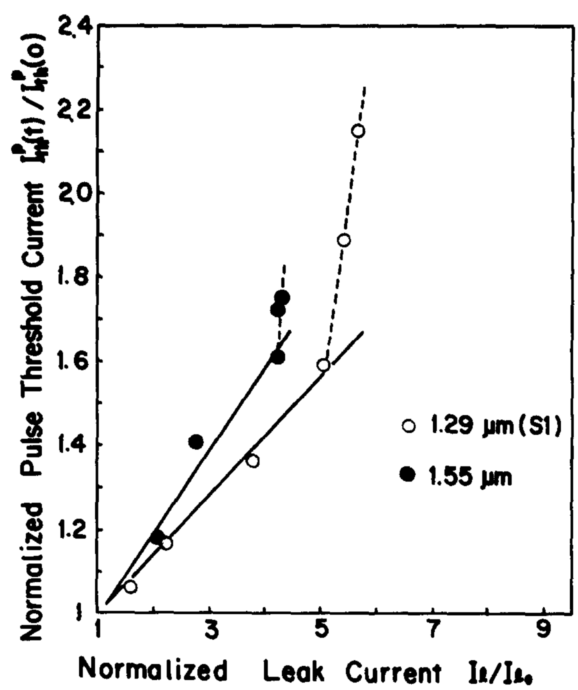

FIG. 3. Typical increase in pulse threshold current vs leak current. Leak currents are plotted at 0.7 V for sample lasing at 1.29 μm and 0.6 V for one lasing at 1.55 μm. Driving current and junction temperature are 10 kA/cm^2 and 250 °C, respectively. The sample of S1 is the same one in Fig. 2.

old currents are closely related with the increment of leak currents within the range where the absorption coefficient is nearly constant and the gain factor is decreasing. Figure 3 shows the typical change of pulse threshold current as a function of recombination ($2kT$ component) leak current. The sample of S1 in Figs. 2 and 3 is the same. The initial current was about 1×10^{-4} A at 0.7 V for the sample lasing at 1.29 μm and at 0.6 V for the sample lasing at 1.55 μm, respectively, and the leak currents were evaluated at those voltages. The leak current of the lasers, which does not degrade under aging, never increased. Therefore, it can be said that the generation of dark defects causes the nonradiative recombination center to increase. In the region where the absorption coefficient begins to increase, a linear relation between the leak current and the pulse threshold current is broken. For the sample denoted S1, there is a kink point on the absorption coefficient versus pulse threshold current relation in Fig. 2 which corresponds to the kink on leak current versus pulse threshold current relation in Fig. 3. The increase of leak current is one of the causes which decreases gain factor. Such behaviors of the absorption coefficient, the gain factor, and the leak current were observed in the degraded samples associated with DSD's as well as with simultaneous DSD's and ⟨100⟩ DLD's appearance. The difference of the degradation mode due to DSD's and ⟨100⟩ DLD's is not clear at present.

From above results, the degradation of lasing characteristics due to DSD's can be divided into two modes. In the initial stage of DSD's generation, DSD's hardly act as an absorber of emitted light, and pulse threshold current increases in proportion to the increase of leak current. In the second stage, DSD's act as an absorber of emitted light. In this region, DSD's become larger and darker in the EL topograph but the number does not change. Although self-sustained pulsation was observed only in samples lasing at 1.29 μm, the degradation modes are similar in samples lasing at 1.29 and 1.55 μm.

In InGaAsP/InP LED's, it was speculated that one of the host atoms, such as In atoms, plays an important role in the generation of DSD's.[2] In the present experiment, a Ga- and As- rich region in an active layer was observed and geometrically correlated with DSD's for samples aged a few hundred hours aging after generation of DSD's.[8] Just after the generation of DSD's, the Ga- or As-rich region was hardly observed or not detected because of a poor sensitivity of an electron probe microanalyzer. The progress of segregation might correspond to the behavior of the absorption coefficient, that is, the absorption coefficient hardly changed at the initial stage of DSD generation and increased during aging after the generation of DSD's. Since DSD's hardly absorb the emitted light just after the generation, DSD's seem to work as a sink of injected carriers rather than as an absorber of emitted light. Injected current concentrated on DSD's.[3] Moreover, as DSD's are generated, the leak current rapidly increases. Therefore, the generation of DSD's is affected mainly by current injection and not by absorption of emitted light. In fact, the generation time of DSD's strongly depended on the magnitude of injected current density as described in Sec. VA.

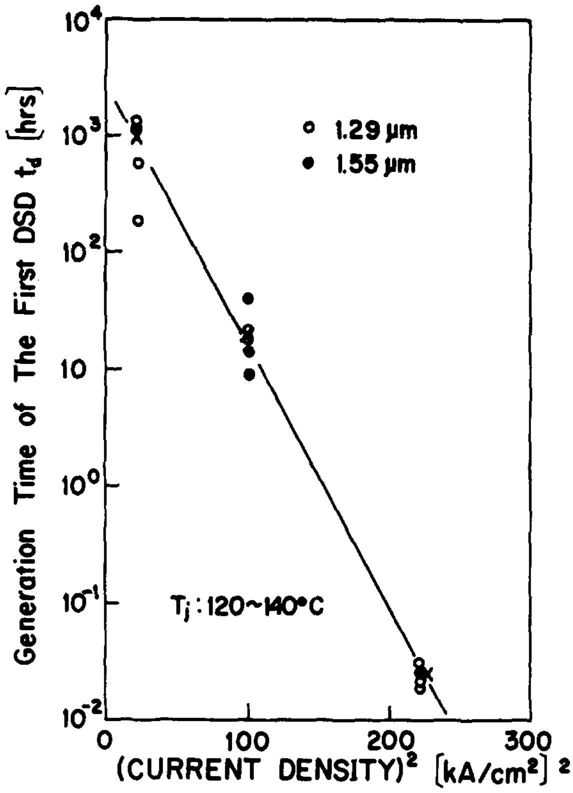

FIG. 4. Generation time of the first DSD as a function of the square of current densities under junction temperature of 120–140 °C. Cross point (X) is the median generation time of the first DSD for each aging condition from the Weibull plot in Fig. 6.

V. DEPENDENCE OF DARK DEFECTS ON AGING CONDITIONS

A. Dark spot defects (DSD's)

Figure 4 shows the relation between the generation time of the first DSD, t_d, and the operating current density. The junction temperatures of samples were adjusted to be between 120 and 140 °C by changing the ambient temperature. The generation time of the first DSD strongly depended on current density, and it can be expressed approximately by the following relation within this experimental range.

$$t_d \propto \exp(-AJ^2), \tag{2}$$

where J is the injected current density and A is a constant.

The generation time for the first DSD, t_d, versus junction temperature at current density of 10 kA/cm^2 is shown in Fig. 5. The generation time becomes short as the junction temperature increases, and an activation energy is estimated to be 0.16 eV. From Figs. 4 and 5, it is clear that the generation time of DSD mainly depends on the injected current densities at the normal operation condition (the current density of 5–10 kA/cm^2 and the junction temperature of 25–100 °C). The effects of injected current become more clear by evaluating the results using Weibull plot in terms of the aging time and the number of samples with DSD's. The Weibull plot of generation time for the first DSD and the cumulative number of the samples with DSD's, which are replotted from Figs. 4 and 5, is shown in Fig. 6. The samples which did not show DSD's throughout the aging were ex-

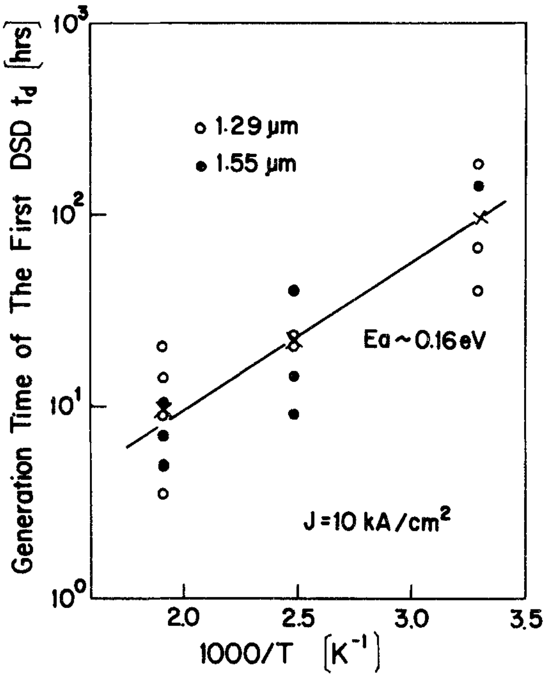

FIG. 5. Generation time of the first DSD as a function of the junction temperature under current density of 10 kA/cm^2. Cross point (X) is the median generation time of the first DSD for each condition from the Weibull plot in Fig. 6.

cluded from statistics. These plots are corrected by median rank. The Weibull shape parameter m weakly depends on the junction temperature as long as current density is constant. On the contrary, m strongly depends on the current density. This means that generation pattern of DSD's as a function of aging time mainly depends on the current density. From the behavior of m value, it is clear that the DSD is generated slowly at low current density and concentrically generated against aging time as current density is high. The generation of these DSD's is the phenomena which are understood in terms of probabilities by the Weibull plot.

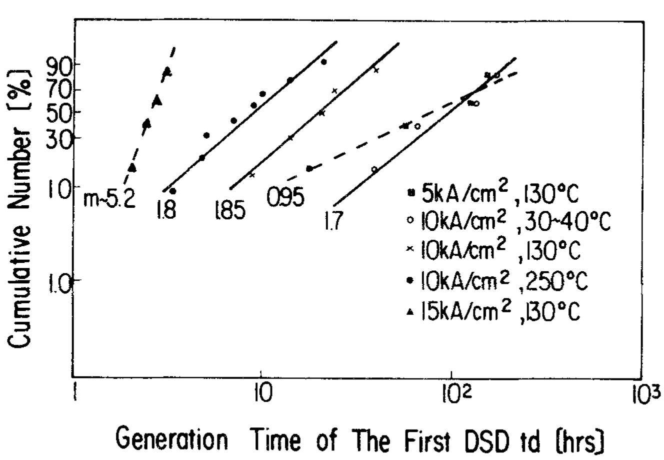

FIG. 6. Weibull plots for generation time of the first DSD, and cumulative number of the sample which appeared in DSD's. Each point is replotted from Figs. 4 and 5. Horizontal axis is multiplied by 10^{-1} for the case of current density of 5 kA/cm^2 and junction temperature of 130 °C (■), and 10^2 for the case of current density of 15 kA/cm^2 and junction temperature of 130 °C (▲).

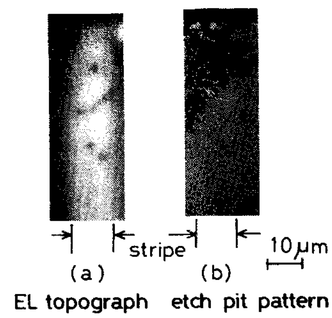

FIG. 7. EL topograph of (a) a sample lasing at 1.29 μm after 200-h aging and (b) the etch-pit pattern at the vicinity of the heteroboundary between the InGaAsP active layer and the p-InP cladding layer. The p-InP cladding layer remains at a thickness of 0.2–0.3 μm on the InGaAsP active layer. Driving current and junction temperature are 10 kA/cm^2 and 250 °C, respectively. Notice that the EL topograph is a mirror image of the etch-pit pattern.

Dependences of DSD generation times on aging conditions described above are quite different from those reported in Ref. 15, where DSD generation time has an activation energy of 1.2 eV. Moreover, in this work the dependence of DSD generation time on current density is much stronger than those reported in Ref. 15. Therefore, different modes may take part in DSD's generation, although the detail mechanism of DSD generation is not known at present.

The generation rate of DSD's depended on wafers, and no DSD's were observed for many samples even after several thousand hours of aging. The dependences of DSD's generation time on current density and temperature are similar in samples lasing at 1.29 and 1.55 μm as shown in Figs. 4 and 5. These facts suggest that the screening of InGaAsP/InP lasers with respect to the DSD's can be carried out by a proper choice of current density and aging time.

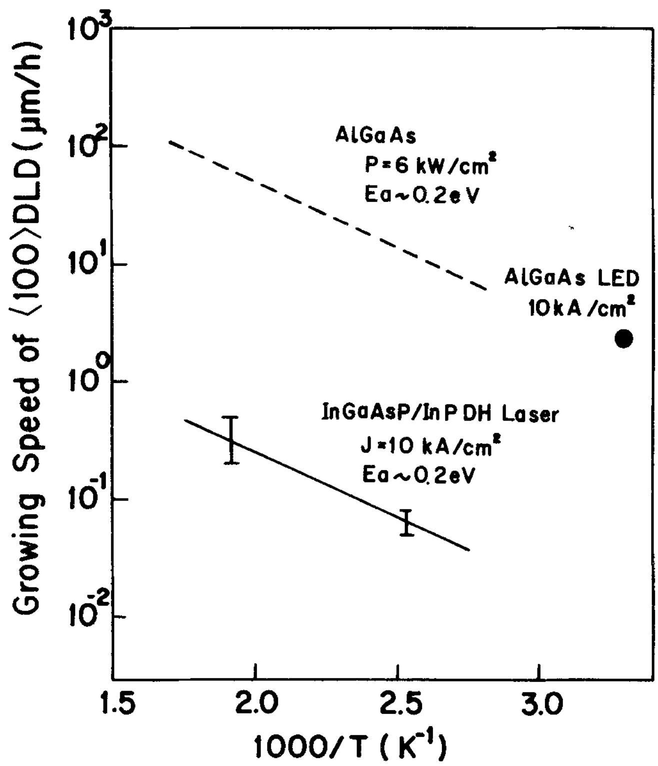

FIG. 8. Growing speed of ⟨100⟩ DLD in samples lasing at 1.29 μm as a function of junction temperature under current density of 10 kA/cm^2. Solid line is this work. Dashed line and closed circle shows the case of AlGaAs material under Kr laser irradiation from Ref. 16 and the datum for AlGaAs/GaAs LED in Ref. 17, respectively.

B. Dark-line defects (DLD's)

In a few samples lasing at 1.29 μm, $\langle 100 \rangle$ DLD's were observed. The $\langle 110 \rangle$ DLD was never observed. An EL topograph of a sample after 200-h aging is shown in Fig. 7(a). The etch-pit pattern in the vicinity of the heteroboundary between the InGaAsP active layer and p-InP cladding layer is also shown in Fig. 7(b). As for this sample, the p-InP cladding layer remained a thickness of 0.2–0.3 μm on the InGaAsP active layer. The etch pits were observed by using a chemical etchant of 1 HBr:3 CH_3COOH. A part of $\langle 100 \rangle$ DLD corresponds to the line-shaped etching pattern, whereas the etch pits corresponding to DSD's are hardly observed in that layer. This fact indicates that the $\langle 100 \rangle$ DLD's exist in the vicinity of heteroboundary between the active layer and the p cladding layer.

The dependence of the growing speed of $\langle 100 \rangle$ DLD's on the junction temperature at a current density of 10 kA/cm^2 is shown in Fig. 8. The activation energy of the growing speed is estimated to be 0.2 eV. This value coincides with that reported on AlGaAs/GaAs DH materials under Kr ion laser irradiation.[16] If the activation energy of 0.2 eV is assumed, the growing speed is estimated to be 10^{-2} μm/h at room temperature. This value is two orders of magnitude smaller than that of AlGaAs/GaAs LED's under similar aging conditions.[17]

VI. SUMMARY

Degradation of InGaAsP/InP DH lasers associated with dark defects was investigated under accelerated aging, and the results can be summarized as follows.

(1) Generation of dark defects in the EL topograph were accompanied with an increase in the pulse threshold current and the leak current. At the initial stage of DSD's generation, these dark defects hardly act as an absorber of emitted light, and the increase in the pulse threshold current was mainly due to the reduction of gain factor. After some degradation, however, dark defects began to act as an absorber of the emitted light.

(2) Generation time of the first DSD strongly depended on the injected current density but only weakly on the junction temperature. The activation energies for the generation time of the first DSD and growing speed of $\langle 100 \rangle$ DLD were estimated to be 0.16 and 0.2 eV, respectively.

(3) The lasers which will degrade by these dark defects could be screened out by a relatively short aging time under high-current injection.

ACKNOWLEDGMENTS

The authors would like to thank Dr. M. Fujimoto and Dr. T. Ikegami for their kind advice, and Dr. H. Nagai, Dr. K. Takehei, and K. Nawata for valuable discussions and supplying DH wafers. Thanks are given to Mr. Y. Suzuki for the fabrication of laser diodes and Mr. M. Seki for observations with the electron probe microanalyzer. They also wish to thank Dr. Y. Kato and Dr. Y. Suemune for their encouragement throughout this work.

[1]T. Yamamoto, K. Sakai, and S. Akiba, IEEE J. Quantum Electron. **QE-15**, 684 (1979).
[2]S. Yamakoshi, M. Abe, O. Wada, S. Komiya, and T. Sakurai, IEEE J. Quantum Electron. **QE-17**, 167 (1981).
[3]M. Fukuda, K. Wakita, and G. Iwane, Jpn. J. Appl. Phys. **20**, L87 (1981).
[4]K. Mizuishi, M. Hirao, S. Tsuji, H. Sato, and M. Nakamura, in Proceedings of the Thirteenth Conference on Solid State Devices, Tokyo, 1981; Jpn. J. Appl. Phys. **21**, 359 (1982), Suppl. 21-1.
[5]K. Ishida, T. Kamejima, Y. Matsumoto, and K. Endo, Appl. Phys. Lett. **40**, 16 (1982).
[6]K. Endo, S. Matsumoto, H. Kawano, I. Sakuma, and T. Kamejima, Appl. Phys. Lett. **40**, 921, (1982).
[7]M. Fukuda, K. Wakita, and G. Iwane, Jpn. J. Appl. Phys. **20**, L153 (1981).
[8]M. Seki, M. Fukuda, and K. Wakita, Appl. Phys. Lett. **40**, 115 (1982).
[9]K. Wakita, H. Takaoka, M. Seki, and M. Fukuda, Appl. Phys. Lett. **40**, 515 (1982).
[10]K. Takahei, H. Nagai, and H. Kawaguchi, Appl. Phys. Lett. **15**, 309 (1980).
[11]B. C. Deloach, Jr., B. W. Hakki, R. L. Hartman, and L. A. D'Asaro, Proc. IEEE **61**, 1042 (1973).
[12]M. Ettenberg and H. Kressel, J. Appl. Phys. **43**, 1204 (1972).
[13]H. Yonez, M. Ueno, T. Kamejima, and I. Sakuma, Jpn. J. Appl. Phys. **13**, 835 (1974).
[14]T. Kobayashi and Y. Furukawa, Jpn. J. Appl. Phys. **14**, 1175 (1975).
[15]S. Yamakoshi, M. Abe, S. Komiya, and Y. Toyama, Tech. Dig. 122 (1979).
[16]H. Imai, T. Fujiwara, K. Segi, M. Takusagawa, and H. Takanashi, Jpn. J. Appl. Phys. **18**, 589 (1979).
[17]S. Yamakoshi, T. Sugahara, O. Hasegawa, Y. Toyama, and H. Takanash, Tech. Dig. 642 (1978).